Time evolution of SBF by electric characterization

F. C. M. Freire[1] · W. R. Weinand[1] · T. M. Andrade[1,2] · J. A. da Cruz[3] · I. Hammami[4] · M. P. F. Graça[4] · P. M. O. Silva[5,6] · A. J. M. Sales[5]

Abstract

Simulated Body Fluid (SBF) for biomedical research, containing several types of ions, is dielectrically characterized by the impedance spectroscopy technique. The real and imaginary parts of the electrical admittance of the SBF are determined by several concentrations of ions dissolved in it. The time dependence of the volume dielectric parameters of the SBF with the frequency indicates an exponential behavior and it is practically independent of the hydroxyapatite (HAp) immersed in it. On the other hand, the surface dielectric parameters show significant differences when the hydroxyapatite was present. Qualitatively, related to chemical kinetic and using the integrated rate law, it was possible to find the half-life time.

Keywords Impedance spectroscopy · SBF · Hydroxyapatite · Dielectric parameters

1 Introduction

Over the last two decades, the research on the Simulated Body Fluid (SBF) has increased. Its utility came from the necessity to substitute the blood in experiments. The human blood plasma has a Ca/P (calcium/phosphorus) molar ratio of 2.50 and pH values between 7.35 and 7.45 [1]. A lot of research was performed in the last years to develop the acellular SBF, with ions concentrations nearly equal to those of human blood plasma [2]. After this research, the scientific community related to the biomaterials field of the opinion

✉ A. J. M. Sales
  jeffsales.brasil@gmail.com

1   Physics Department, State University of Maringá, Maringá, PR 87020-900, Brazil

2   Cesumar Institute of Science, Technology and Innovation, Maringá, PR 87050-390, Brazil

3   Department of Environment, State University of Maringá, Umuarama, PR 87020-900, Brazil

4   i3N and Physics Department, University of Aveiro, 3810-193 Aveiro, Portugal

5   Laboratório de Telecomunicações e Ciências e Engenharia de Materiais (LOCEM), Physics Department, Federal University of Ceara, Fortaleza, CE 60020-181, Brazil

6   Department of Electrical/Mechanical Engineering, Unime Faculty of Exact and Technological Sciences, Campus Lauro de Freitas, Lauro de Freitas 42702-420, Brazil

that the apatite formation on a material immersed in SBF is proof of their bioactivity and can be used to predict their binding capacity in vivo bone [3]. In 2003, due to the difficulty of preparing the SBF without precipitation, a refined recipe was proposed as a standard solution for studies in vitro apatite forming ability of implant materials [4]. Apatite formation on the surface of a material immersed in SBF depends on the conditions of its surface and factors related to fluid, such as pH, temperature, immersion time, renewal of fluid, nature of immersion (static or dynamic), and ionic concentration. These factors could influence the results of in vitro tests. The ionic concentration (Ca^{2+}, PO_4^{3-}) present in the SBF should be monitored by chemical analysis, since these fluids a metastable solution supersaturated concerning apatite [5, 6]. The state of the SBF can also be checked by immersion (for short time) in materials that exhibit high bioactivity index (IB) as the 45S5 bioglass or medium index of bioactivity as the AW Cerabone, Ceravital and Hydroxyapatite followed by scanning electron microscopy (SEM) and energy dispersive spectroscopy (EDS) [7]. Hydroxyapatite $[Ca_{10}(PO_4)_6(OH)_2]$ belongs to the bioactive biomaterial category and is the main mineral component of hard bone tissues. This ceramic remains chemically stable in the physiological middle and induces specific biological activity [8–12]. In general, the quality of SBF is verified after the immersion of bioactive materials for some days in SBF, such materials present growth of apatite on their surface. This growth may be characterized by several techniques, mainly

by SEM followed by EDS. However, testing the quality of SBF by verifying the apatite growth after immersion generally requires several days and only shows whether there is apatite film formation, neglecting other aspects that could affect the SBF quality. In this sense, Fojt et al. [13] developed a method applying impedance spectroscopy methods for online measuring the apatite layer formation demonstrating that it can be a useful method for online measuring the layer formation. In essence, such kinds of measurements can also be used to check the quality of SBF by performing impedance spectroscopy measurements over time to track the dynamics of ions contained in the SBF during the formation of the apatite layer on a well-known bioactive sample, such as hydroxyapatite. Indeed, electrical conduction in electrolytic cells has been widely used to investigate the role of the ions. In general, the aim is to investigate the frequency dependencies of the real and imaginary parts of the impedance of a sample in the shape of a slab, of ionic solutions. Particular attention is devoted to the SBF when is evolving in time [14–16]. This work aims to explore, from the dielectric point of view, the quality of SBF using the Impedance Spectroscopy (IS) Technique. Some models have been used to understand the basic mechanisms in simulated body fluids [15–19]. Equivalent circuit models have long been used to model the interface impedance; and here our focus is to study the time-dependent evolution of the SBF during a biomaterial immersion. Theories and experiments have shown that the electrodes play a fundamental role in the impedance measurements, and this will also be taken into consideration [20].

2 Materials and methods

The conventional SBF was prepared according to the protocol adopted by Kokubo et al. [21]. Typically, the reagents NaCl, KCl, NaHCO$_3$, MgCl$_2$6H$_2$O, CaCl$_2$, Na$_2$SO$_4$, and K$_2$HPO$_4$3H$_2$O were dissolved into deionized water and buffered at pH $= 7.4$ with Tris-buffer and HCl 1.0 M at 36.5 ± 0.5 °C. The SBF presents the following ionic concentration in mM: Na$^+$ 142.0, K$^+$ 5.0, Mg^{2+} 1.5, Ca^{2+} 2.5, Cl$^-$ 147.8, HCO$_3^-$ 4.2, HPO$_4^{2-}$ 1.0, SO$_4^{2-}$ 0.5, similar to those of the human blood plasma. The solution was filtered through a 0.2 μm pore size syringe filter before the experimental work. Three cases were analyzed: labeled as Ch0 only SBF; labeled as Ch1 SBF plus HAp and labeled as Ch2 SBF plus HAp with the renewing of SBF solution every 4 days. The samples were soaking in SBF for 28 days. Natural hydroxyapatite used in this study was produced via calcination of fish bones from Brazilian rivers according to previous reports [8–12]. Figure 1A, B shows, respectively, the HAp surface morphology before immersion and the semiquantitative elemental analysis by EDS, which reveals

the presence of the elements Ca, P and O characteristic of HAp with a molar ratio (Ca/P) of about 1.65. The HAp surface morphology after immersion is shown in Fig. 1C. The formation of an apatite layer characteristic of the nucleation and growth of apatite in SBF solution is observed. The EDS analysis is shown in Fig. 1D and reveals the presence of the elements Ca, P and O that make up HAp and a Ca/P ratio around 1.58.

The dielectric properties of the SBF have been determined utilizing the dielectric spectroscopy technique [17] using a Solartron 1260 Impedance/Gain-Phase Analyzer. The SBF samples were submitted to an external periodic voltage, and the admittance was measured. When applied small amplitude voltage, $V_0 = 25$ mV, the cell behaves as a linear system, and the electrical admittance, Y, of the cell is independent of V_0 [22]. The frequency range used was from 1 Hz to 1 MHz. The data were acquired with appropriate software modified by us. From the analysis of the real, G, and imaginary, B, parts of Y, versus the frequency of the applied voltage, $f = \omega/2\pi$, it is possible to find an equivalent representation in form of Resistor, Inductor, and Capacitor (RLC) circuits. We have performed the measurements of impedance spectroscopy on several samples; but only the most significant ones are presented, labeled as blank SBF, named Ch0; SBF plus hydroxyapatite, Ch1; and SBF plus hydroxyapatite, where the SBF was renewed every 4 days, cited along with the text as Ch2. The sample holder has a circular shape (of radius $r = 10$ mm) of parallel plates, separated by fixed thickness. The electrodes were made with stainless steel. The thickness of the sample, d, considered in our measurement's ranges between 0.5 and 1.0 mm. The stainless-steel electrodes were immersed in the SBF, held by a plastic bottle (Fig. 2).

After 28 days of measurements, it was found that there is no apatite nucleation in the electrode plates, verified with SEM for the stainless-steel electrodes, see one surface example in Fig. 3. Inside the plastic bottle, the used volume was 50 ml. Typical HAp sample dimensions were 10 mm in diameter and 1.5 mm in thickness. All measurements have been made in a controlled temperature bath at 36.5 ± 0.5 °C and hermetically sealed.

3 Standard admittance behavior of the SBF

The behavior of the conductivity spectrum derived by $G = R(Y)$ and $B = I(Y)$, reported in Fig. 4, are, respectively, the conductance and the susceptance. This figure indicates the presence of one more sensible region (around 103 Hz). Figure 4 shows the amount of 28 days of measurement, ranging from blue to red color curves. The figure shows the behavior of the pure SBF without the fluid renewing (Ch0).
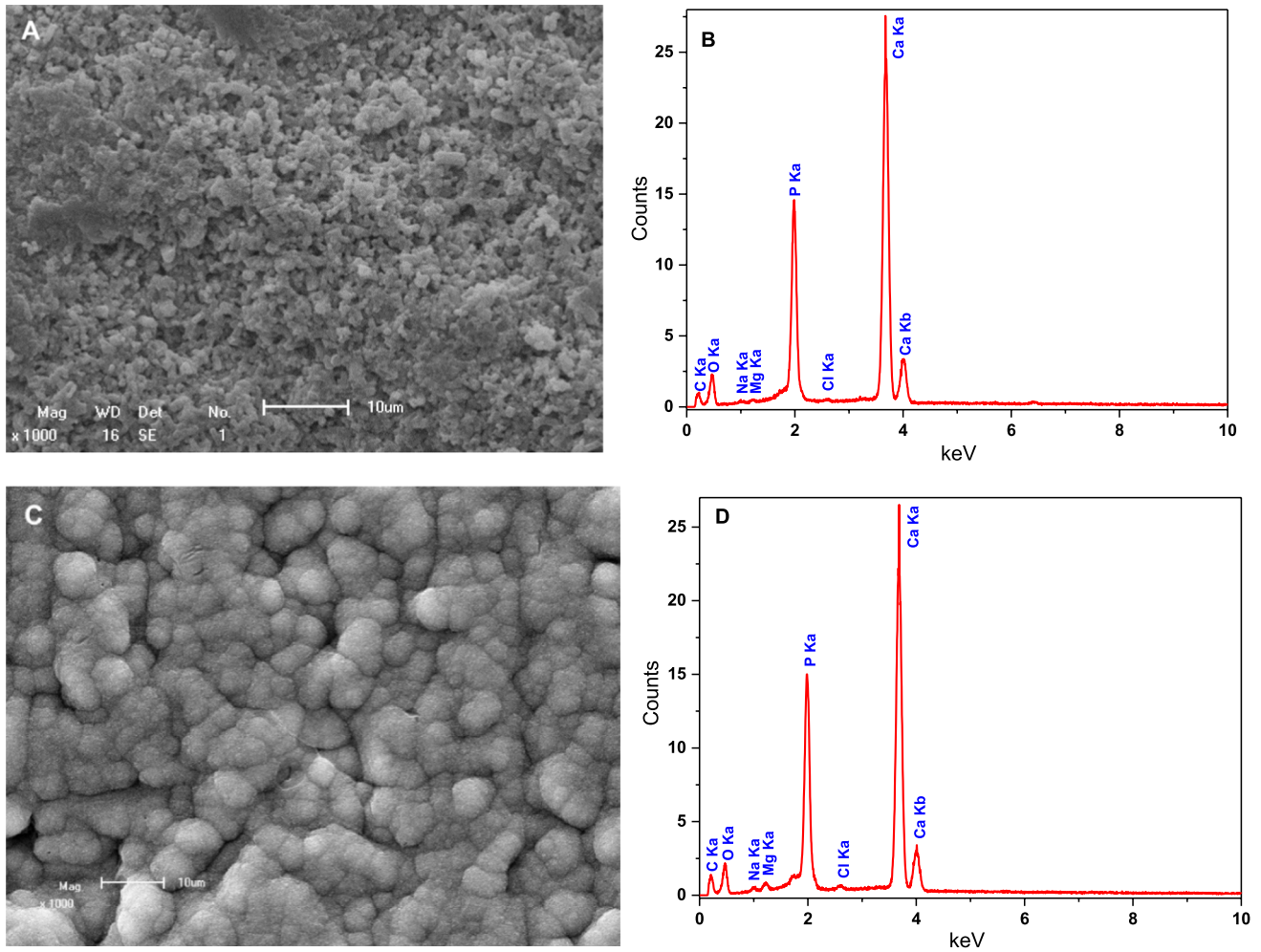
Fig. 1 A, B SEM image of the HAp surface and the EDS spectrum, before immersion in SBF, respectively. **C, D** SEM image of the HAp surface and the respective EDS spectrum, after immersion in SBF showing the morphology of the apatite layer formed after 28 days of immersion
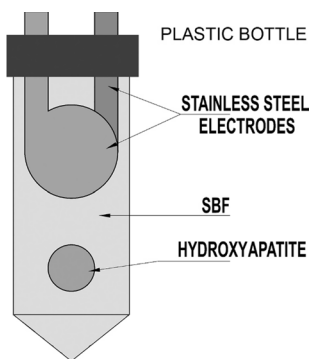

**Fig. 2** Sample holder with stainless steel electrodes and HAp sample in imersion in SBF

Conversely, Fig. 5 shows the amount of 28 days of measurement, ranging from blue until red color. The sample holder was filled with SBF plus a HAp. In the same way, this second set was measured without SBF replacement (Ch1).
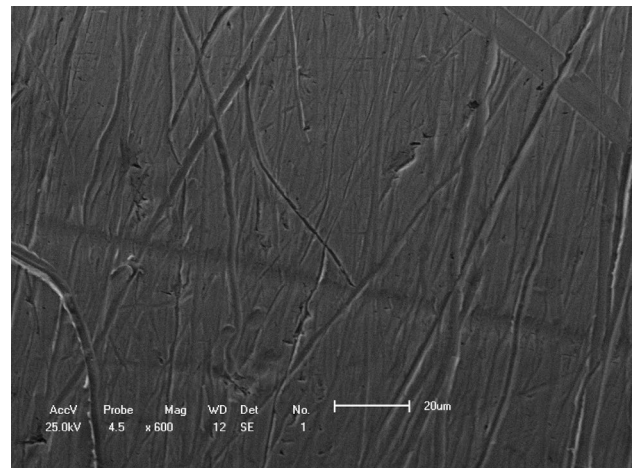

Fig. 3 Scanning electron microscopy of the stainless steel electrodes surface after immersion in SBF for 28 days
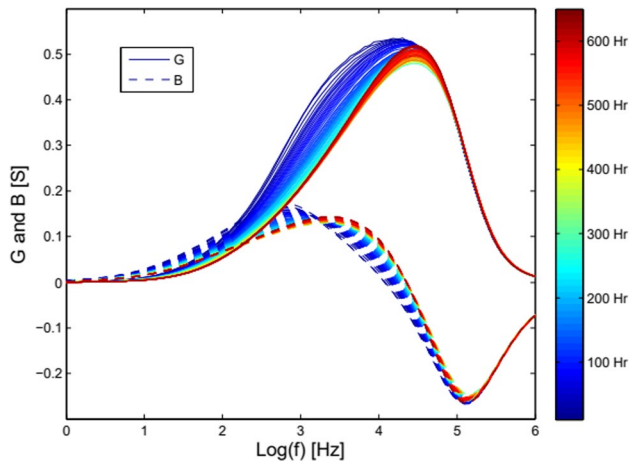
Fig. 4 Frequency dependence of the real, *G*, and imaginary, *B*, parts of the electrical impedance of cells filled with SBF. The right colored bar represents the time evolution
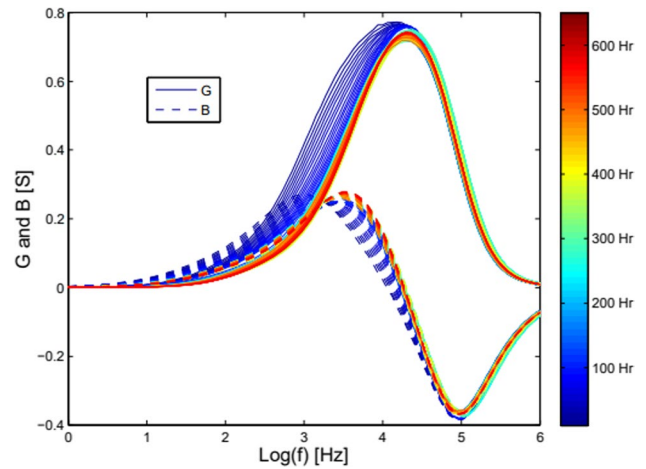
Fig. 6 Frequency dependence of the real, *G*, and imaginary, *B*, parts of the electrical impedance of cells filled with pure SBF plus HAp. SBF is renewed every 4 days. The right colored bar represents the time evolution
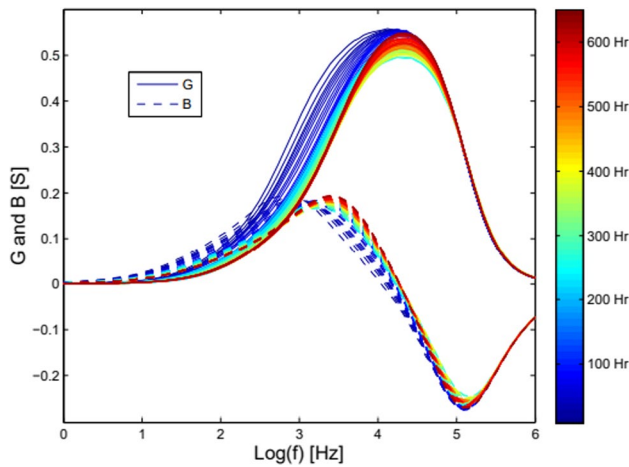
Fig. 5 Frequency dependence of the real, *G*, and imaginary, *B*, parts of the electrical impedance of cells filled with pure SBF plus HAp. The right colored bar represents the time evolution

And finally, we can see the admittance behavior of SBF plus HAp, where the SBF was renewed every 4 days in Fig. 6 (Ch2).

4 Dielectric characterization using some models

4.1 Simple RLC circuit model

From the analysis of the real, *G*, and imaginary, *B*, parts of admittance $Y = 1/Z$, versus the frequency of the applied voltage, $f = \omega/2\pi$, it is possible to determine the dielectric behavior using an equivalent circuit composed by RLC

components. The first model proposed an equivalent circuit composed of a parallel circuit representing the bulk interaction (R_b and C_b); in series, a capacitance (C_s), an inductance (L_s), and a resistance (R_s). The circuit impedance can be written as

$$Z = \frac{1}{Y} = \frac{1}{i\omega C_s} + \frac{R_b}{1 + i\omega R_b C_b} + R_S + i\omega L_S. \tag{1}$$

4.2 RLC circuit model with CPE impedance

As described by Alexe-Ionescu et al. [23], with ionic solutions in the low-frequency region, the frequency dependencies of the impedance are well-described by assuming that the electrodes are responsible for an impedance described by

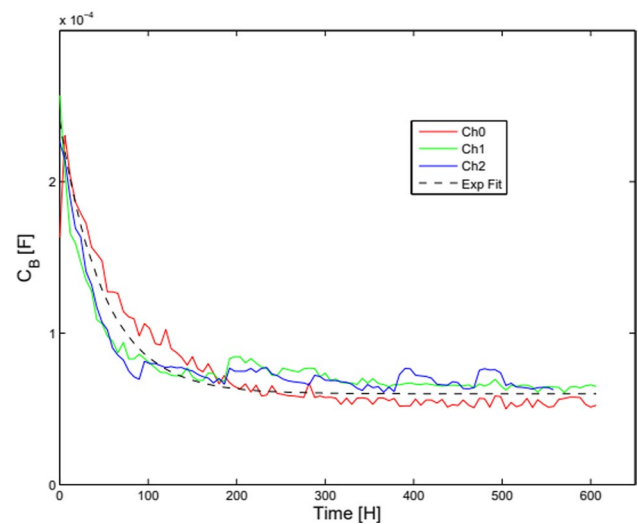$$Z_{\text{int}} = \frac{1}{A(i\omega)^p}, \tag{2}$$

where *A* and $p \leq 1$ are two constants and Z_{int} is known as the Constant Phase Element (CPE), introduced by Cole and Cole [24]. In this case, the total electrical impedance, $Z = 1/Y$, is the sum of the bulk electrical impedance contribution, Zb, and Z_{int}. In our case, we have proposed

$$Z = \frac{1}{Y} = \frac{R_b}{1 + i\omega R_b C_b} + i\omega L_S. \tag{3}$$

The inductance element has been introduced as described by Sanabria and Miller [19], probably to interpret the setup cables and connections.
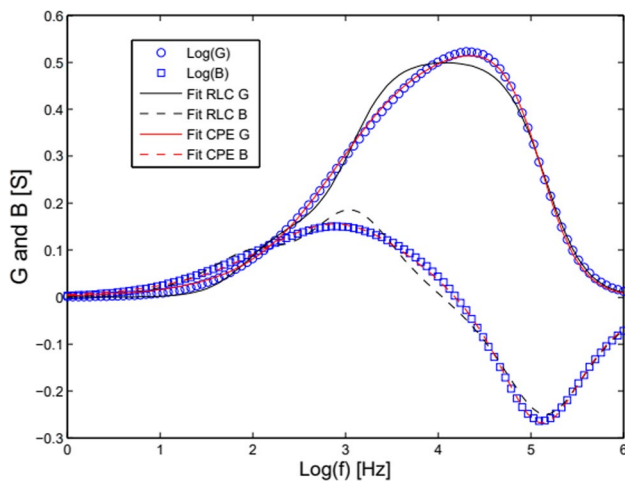
Fig. 7 Frequency dependence of the real, G, and imaginary, B, parts of the electrical impedance of cells filled with pure SBF, and the fits using the RLC model and the RLC plus CPE model

Table 1 Representative values of the significant parameters involved in the RCL model fitting (Eq. 1)

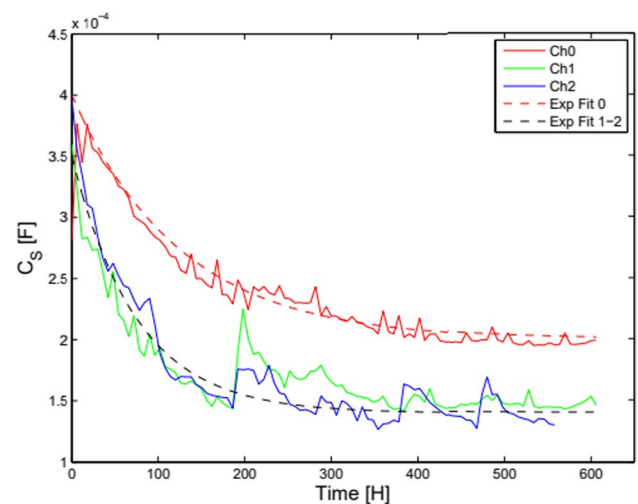| Parameter	Symbol	Ch0	Ch1	Ch2
Bulk resistance [Ω]	R_b	4.0	4.5	4.5
Serie resistance [Ω]	R_s	2.1	2.0	1.5
Serie inductance [μH]	L_s	2.3	2.3	2.3

5 Experimental results

A Genetic Algorithm program was used to fit the experimental data. Details can be found in Scalerandi et al. [25]. The models used in this fit were mentioned above in Eqs. 1 and 3. Figure 7 shows an example of the fit using the RLC model and the RLC plus CPE model. The curves using CPE models fit better.

Using the single RLC model (Eq. 1) we have obtained, for the three cases, the parameters as they can be seen in Table 1.

The other parameters have presented softly exponential behavior. Figure 8, the bulk capacitance, presents an exponential decay.

It is possible to see that the bulk contribution (Rb and Cb), despite the exponential capacitance decay, was the same in all cases (channels), which leads us to believe that the main differences are surface contributions, such us surface capacitance Cs, as shown in Fig. 9.

On the other hand, using the RLC–CPE model (Eq. 3) we have obtained, for the three cases, the following constant parameters, as can be seen in Table 2.

Fig. 8 Temporal dependence of parallel bulk capacitance. Ch0 means pure SBF; Ch1 means SBF plus HAp and Ch2 means SBF plus HAp renewed every 4 days

Fig. 9 Temporal dependence of series bulk capacitance. Ch0 means pure SBF; Ch1 means SBF plus HAp and Ch2 means SBF plus HAp renewed every 4 days

Table 2 Representative values of the significant parameters involved in the RCL + CPE fitting (Eq. 3)

Parameter	Symbol	Ch0	Ch1	Ch2
Bulk resistance [Ω]	R_m	1.82	1.78	1.25
Bulk capacitance [nF]	C_m	0.16	0.18	0.16
Inductance [μH]	L_s	2.3	2.3	2.3
CPE power	p	0.65	0.70	0.74
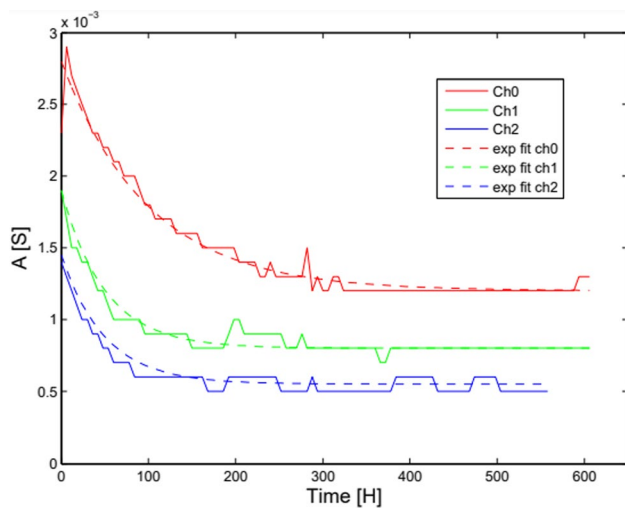
Fig. 10 Temporal dependence of CPE parameter. Ch0 means pure SBF; Ch1 means SBF plus HAp and Ch2 means SBF plus HAp renewed every 4 days

Table 3 Representative values of the significant parameters involved in the time exponential decay fits

Parameter	a [mS]	b [h]	c [mS]
C_B (All channels)	18.0	50	6.0
C_S (Ch0)	20.0	125	20.0
C_S (Ch1–Ch2)	20.0	75	14.0
A (Ch0)	1.60	100	1.20
A (Ch1)	1.10	50	0.80
A (Ch2)	0.90	50	0.55

The value of LS can be related to the electrical inductance of the cables. The other parameters have presented different exponential behavior. Figure 10 shows us an exponential decay for the A variable CPE model. We have proposed a time exponential decay of type $f(t) = ae^{-t/b} + c$. In the CPE case, we can write the A CPE parameter as

$$A(t) = ae^{-\frac{t}{b}} + c. \tag{4}$$

Table 3 shows us that the time decay (b) in the pure SBF is slower than in the SBF plus HAp in both fits.

The time constant, in both models, is twice slower than when the HAp is immersed in the SBF, suggesting that it interacts with the ions for the apatite nucleation. In addition, we can see (in Table 3) that, in the first model, the time constant for the surface capacitance is slower for Ch0 than for Ch1 and Ch2. The time constant for the bulk contribution is the same for the three cases, proposing that the surface elements govern the effects of ionic contribution.

In similar work, Sanabria et al. [19], show that the called "fractal dimension" p is different for distinctions used in the solution. This means that, in our case, when the apatite has grown on the hydroxyapatite surface, there are different concentrations of ions for the three cases. The p values for the ch0 are smaller than those for the ch1 and ch2. Is expected that the A behavior is similar to the conductivity σ, multiplied by the geometric factor d/S. These results are shown in Fig. 10.

The calcium and phosphate ions concentrations decrease in the SBF when the apatite its forming. In Miyazaki et al. work [19], they show variations in the element concentrations of SBF as a function of soaking time in Treated Tantalum metal by Inductively Coupled Plasma (ICP). They show, in the SBF, a steep increase in Na concentration, and a large decrease in the calcium and phosphate ions concentrations as a time function, which is explained by changes in the concentration induced by the apatite nucleation. On the sample surface, a large amount of calcium and phosphate ions was adsorbed to form the apatite. In the same way, AlexeIonescu et al. [18] show that the conductivity equivalent of KCl and NaCl is directly proportional to the ionic concentration. Therefore, if the conductivity is proportional to the concentrations of the ions, the results show that, with the growth of the apatite, the conductivity decreases in time. Chemical kinetics is the quantitative study of chemical systems that are changing with time. Usually, the reactions throughout time are proportional to the changes in concentrations of the reactants and products, i. e. the rate k is proportional to a time derivative of a concentration. Suppose that this reaction obeys a first-order rate law, this rate law can also be written as

$$k[C] = -\frac{d[C]}{dt}, \tag{5}$$

where [C] is the concentration of a reactant or product. Integration of Eq. 5 produces the corresponding integrated rate law,

$$[C] = [C]_0 e^{-kt}, \tag{6}$$

which relates the concentration to time [26, 27]. Qualitatively, it is possible to confront the exponential behavior, the bulk capacitance (CB), the series capacitance (CS), and the A parameter with the integrated rate law cited above. This leads us to conclude that the rate k, in confront to the results, ranging from 0.008 to 0.02 h^{-1}, as it is possible to see in Table 3, is $b \approx 1/k$. This rate gives us a description of how fast a reaction is occurring, and the half-life provides an approximate measure of the reaction rate. In this case, the half-life is $t^{1/2} = \ln(2)/k$, ranging from 35 to 90 h approximately.

6 Conclusions

The impedance spectroscopy measurements have been performed on samples with different conditions: pure SBF, SBF plus HAp and SBF plus HAp with fluid renewal every 4 days. The measurements have been performed for approximately 600 h, with an admittance curve being collected every hour for three different setups. Two models corresponding to the equivalent circuit models have been used to quantify the electrode–electrolyte interface and separate the bulk from the surface contribution. The time behavior of the admittance was presented and, using the integrated rate law was possible to find, qualitatively, the half-life time. Because, right after the SBF synthesis, it can be checked with the impedance spectroscopy without being required days to verify the growth of the apatite in bone samples.

Data availability The raw/processed data required to reproduce these findings cannot be shared at this time as the data also forms part of an ongoing study.

Declarations

Conflict of interest The authors declare that they have no known competing financial interests or personal relationships that could have appeared to influence the work reported in this paper.

References

1. A.C. Tas, X-ray-amorphous calcium phosphate (acp) synthesis in a simple biomineralization medium. J. Mat. Chem. B **1**(35), 4511–4520 (2013)
2. T. Kokubo, H. Kushitani, S. Sakka, T. Kitsugi, T. Yamamuro, Solutions able to reproduce in vivo surface-structure changes in bioactive glass-ceramic aw3. J. Biomed. Mater. Res. **24**(6), 721–734 (1990)
3. M. Bohner, J. Lemaitre, Can bioactivity be tested in vitro with sbf solution? Biomaterials **30**(12), 2175–2179 (2009)
4. M.R.T. Filgueiras, G. La Torre, L.L. Hench, Solution effects on the surface reactions of three bioactive glass compositions. J. Biomed. Mater. Res. **27**(12), 1485–1493 (1993)
5. T. Kokubo, H. Takadama, How useful is sbf in predicting in vivo bone bioactivity? Biomaterials **27**(15), 2907–2915 (2006)
6. C. Zhao, X. Zhu, T. Yuan, H. Fan, X. Zhang, Fabrication of biomimetic apatite coating on porous titanium and their osteointegration in femurs of dogs. Mater. Sci. Eng. C **30**(1), 98–104 (2010)
7. W. Cao, L.L. Hench, Bioactive materials. Ceram. Int. **22**(6), 493–507 (1996)
8. W. Lima, W. Weinand, O. dos Santos, A. Paesano, F. Ortega, Effect of the calcination time of fish bones in the synthesis of hydroxyapatite. Mater. Sci. Forum **498**, 600–605 (2005). (**Trans Tech Publ**)
9. T. Coelho, E. Nogueira, A. Steimacher, A. Medina Neto, W.R. Weinand, W.M. Lima, M. Baesso, A. Bento, Characterization of natural nanostructured hydroxyapatite obtained from the bones of Brazilian river fish. J Appl. Phys. **100**(9), 094312 (2006)
10. T. Coelho, E. Nogueira, W.R. Weinand, W.M. Lima, A. Steimacher, A. Medina-Neto, M.L. Baesso, A.C. Bento, Thermal properties of natural nanostructured hydroxyapatite extracted from fish bone waste. J. Appl. Phys. **101**(8), 084701 (2007)
11. W.R. Weinand, A.C. Bento, M.L. Baesso, W.M. Lima, Numerical approach to determine the elastic modulus of sintered natural hydroxyapatite. J. Appl. Phys. **104**(8), 083711 (2008)
12. J.A. Da Cruz, W.R. Weinand, A.M. Neto, R.S. Palácios, A.J.M. Sales, P.R. Prezas et al., Low-cost hydroxyapatite powders from Tilapia fish. JOM (2020). https://doi.org/10.1007/s11837-019-03998-4
13. J. Fojot, L. Joska, V. Hybasek, E. Pruchova, J. Malek, Impedance technique for monitoring of apatite precipitation from simulated body fluid. Electrochemical Acta **271**, 158–164 (2018)
14. J.R. Mc Donald, Theory of space-charge polarization and electrode-discharge effects. J. Chem. Phys. **58**(11), 4982–5001 (1973)
15. J.R. Mc Donald, J. Garber, Analysis of impedance and admittance data for solids and liquids. J. Electrochem. Soc. **124**(7), 1022–1030 (1977)
16. J.R. Mc-Donald, Impedance spectroscopy: models, data fitting, and analysis. Solid State Ionics **176**(25), 1961–1969 (2005)
17. J.R. Mc Donald, Three to six ambiguities in immittance spectroscopy data fitting. J. Phys. Condens. Matter **24**(17), 175004 (2012)
18. G. Barbero, A. Alexe-Ionescu, Role of the diffuse layer of the ionic charge on the impedance spectroscopy of a cell of liquid. L. Cryst. **32**(7), 943–949 (2005)
19. H. Sanabria, J.H. Miller Jr., Relaxation processes due to the electrode-electrolyte interface in ionic solutions. Phys. Rev. E **74**(5), 051505 (2006)
20. T. Miyazaki, H.M. Kim, T. Kokubo, C. Ohtsuki, H. Kato, T. Nakamura, Mechanism of bonelike apatite formation on bioactive tantalum metal in a simulated body fluid. Biomaterials **23**(3), 827–832 (2002)
21. ISO 23317; Implants for surgery - In vitro evaluation for apatite forming ability of implant materials, International Standard, 2007.
22. G. Barbero, A. Alexe-Ionescu, I. Lelidis, Significance of small voltage in impedance spectroscopy measurements on electrolytic cells. J. Appl. Phys. **98**(11), 113703 (2005)
23. A. Alexe-Ionescu, G. Barbero, F. Freire, R. Merletti, Effect of composition on the dielectric properties of hydrogels for biomedical applications. Physiol. Meas. **31**(10), S169 (2010)
24. K.S. Cole, R.H. Cole, Dispersion and absorption in dielectrics i. alternating current characteristics. J. Chem. Phys. **9**(4), 341–351 (1941)
25. P.P. Delsanto, A. Romano, M. Scalerandi, F. Moldoveanu, Application of genetic algorithms to ultrasonic tomography. J. Acoust. Soc. Am. **104**(3), 1374–1381 (1998)
26. C. Capellos, B. H. J. Bielski, Kinetic systems: mathematical description of chemical kinetics in solution (Wiley-Interscience, 1972)
27. K.A. Connors, *Chemical kinetics: the study of reaction rates in solution* (John Wiley & Sons, 1990)